Molecules and Cells

Rapid Report

MS2 Labeling of Endogenous Beta-Actin mRNA Does Not Result in Stabilization of Degradation Intermediates

Songhee H. Kim[1,2], Melissa Vieira[2,3], Hye-Jin Kim[2], Mahipal Singh Kesawat[2], and Hye Yoon Park[1,2,3,4,*]

[1]Department of Physics and Astronomy, [2]Institute of Molecular Biology and Genetics, [3]Interdisciplinary Program in Neuroscience, [4]Institute of Applied Physics, Seoul National University, Seoul 08826, Korea
*Correspondence: hyeyoon.park@snu.ac.kr
http://dx.doi.org/10.14348/molcells.2019.2398
www.molcells.org

The binding of MS2 bacteriophage coat protein (MCP) to MS2 binding site (MBS) RNA stem-loop sequences has been widely used to label mRNA for live-cell imaging at single-molecule resolution. However, concerns have been raised recently from studies with budding yeast showing aberrant mRNA metabolism following the MS2-GFP labeling. To investigate the degradation pattern of MS2-GFP-labeled mRNA in mammalian cells and tissues, we used Northern blot analysis of β-actin mRNA extracted from the *Actb-MBS* knock-in and MBS×MCP hybrid mouse models. In the immortalized mouse embryonic cell lines and various organ tissues derived from the mouse models, we found no noticeable accumulation of decay products of β-actin mRNA compared with the wild-type mice. Our results suggest that accumulation of MBS RNA decay fragments does not always happen depending on the mRNA species and the model organisms used.

Keywords: β-actin mRNA, mouse, MS2-GFP system, Northern blot, single RNA imaging

INTRODUCTION

In the past two decades, numerous RNA tagging methods have been developed for live-cell imaging of RNA molecules (reviewed in (Moon et al., 2016; Rath and Rentmeister, 2015)). Among them, the MS2-GFP system, using the highly specific interaction between the MS2 coat protein (MCP) and the MS2 binding site (MBS) (Beach et al., 1999; Bertrand et al., 1998), has been widely used for single mRNA imaging. In the MS2-GFP system, a target mRNA is tagged with multiple repeats of MBS, and MCP fused with a fluorescent protein (MCP-FP) is co-expressed in the same cell. The number of MBS repeats directly determines the amplification factor of the signal; 24 repeats of MBS are commonly used for single RNA tracking with a high signal-to-noise ratio (SNR) (Fusco et al., 2003; Park et al., 2010). This method enables the monitoring of dynamic changes in mRNA transcription, localization, translation, and decay within live cells (reviewed in (Tutucci et al., 2018a; Vera et al., 2016)).

However, concerns have been recently raised about possible artifacts of the MS2-GFP system when used in *Escherichia coli* (*E. coli*)(Golding and Cox, 2004) and *Saccharomyces cerevisiae* (*S. cerevisiae*)(Garcia and Parker, 2015; 2016; Haimovich et al., 2016; Heinrich et al., 2017). The tight binding between MBS and MCP may hinder the proper degradation of the tagged mRNA, which could lead to the accumulation of mRNA decay fragments. This raises an important issue because it can complicate the interpretation of live-cell imaging data for monitoring the dynamics of

Received 2 October, 2018; revised 17 January, 2019; accepted 5 February, 2019; published online 27 February, 2019

eISSN: 0219-1032

mRNA movement and associated processes. In this context, Garcia and Parker presented evidence that MBS stem-loops bound by MCP block the exonuclease XrnI activity on the mRNA substrate in budding yeast strains (Garcia and Parker, 2015). By using Northern blot analysis, they examined the degradation patterns of the MBS-tagged *QCR8* and *PGK1* mRNAs expressed from TET-off plasmids and the endogenous *MFA2* and *ASH1* mRNAs labeled with the MBS cassette knocked in the 3′ untranslated region (UTR). In this study, a substantial accumulation of 3′ mRNA fragments containing the MBS was observed when MCP-3×GFP was co-expressed in the yeast cells. This population of mRNA decay fragments hybridized to the probes targeting the 3′ side of the MBS array and required the cytoplasmic 5′ to 3′ exonuclease XrnI for its accumulation.

Supporting Garcia and Parker, Heinrich *et al.* also reported that the introduction of the MBS or its orthologous PP7 binding site (PBS) stem-loops can affect the processing and localization of *PGK1* mRNA in budding yeast (Heinrich et al., 2017). Using single molecule fluorescence in situ hybridization (smFISH), they found that 3′-end stem-loop-containing fragments accumulate in processing bodies (P-bodies) and that the number of nascent mRNAs increases upon stem-loop tagging in glucose-depleted conditions. PBS-tagged *FBA1* and *GFA1* mRNAs also showed a similar aberrant enrichment in the P-bodies. However, the increase in the nascent mRNA number was observed only for the abundant mRNA species, such as *PGK1* and *FBA1* mRNAs, but not for the moderately expressed mRNAs, such as *GFA1* mRNA.

Based on RNA-binding protein purification and identification (RaPID) (Slobodin and Gerst, 2010) and real-time quantitative polymerase chain reaction (RT-qPCR) experiments, Haimovich *et al.* noted that the accumulation of 3′ decay products may not be a general phenomenon for endogenously expressed MS2-tagged mRNAs; rather, it could be an artifact arising from the overexpression of the tagged mRNAs (Haimovich et al., 2016). However, Northern blot analysis still detected 3′ decay fragments from several endogenously expressed MS2-labeled mRNAs in yeast (Garcia and Parker, 2016). Yet, it is still an open question whether this result can be generalized to other mRNAs and other organisms.

As a case study in a mammalian system, we have examined the endogenously expressed MBS-tagged β-actin mRNA using *Actb-MBS* (Lionnet et al., 2011) and MBS×MCP mice (Park et al., 2014). The *Actb-MBS* and MBS×MCP mice have been extensively used to investigate transcription (Cho et al., 2016; Kalo et al., 2015; Lionnet et al., 2011), nuclear export (Grunwald and Singer, 2010), nuclear and cytoplasmic transport (Lee and Park, 2018; Monnier et al., 2015; Park et al., 2014; Smith et al., 2015; Song et al., 2018), protein-RNA interactions (Eliscovich et al., 2017; Wu et al., 2015), and localization and local translation of β-actin mRNA (Buxbaum et al., 2014; Katz et al., 2012; 2016; Park et al., 2012; Yoon et al., 2016). We used Northern blot analysis following the approach used for budding yeast (Garcia and Parker, 2015) and found no noticeable accumulation of 3′ decay products containing the MBS in either mouse embryonic fibroblasts (MEFs) or various organ tissues from the mouse models. Our results suggest that the *Actb-MBS* and MBS×MCP mice can be used without concern for possible accumulation of MBS RNA decay fragments.

MATERIALS AND METHODS

Animals

Animal care and experiments were performed in accordance with the protocols approved by the Institutional Animal Care and Use Committee (IACUC) at Seoul National University. The *Actb-MBS* knock-in and MBS×MCP hybrid mouse models were housed under specific-pathogen-free (SPF) conditions in the research animal facility at Seoul National University. For comparison of different organs, 3-8-week-old male mice were used.

Tissue cultures

The wild-type (WT) and *Actb-MBS* MEFs were cultured from E14 embryos and immortalized by transfecting a plasmid expressing SV40 large T antigen as described previously (Lionnet et al., 2011). The MBS×MCP MEF cell line was generated by infecting the *Actb-MBS* MEF with a lentiviral vector expressing MCP-GFP under the ubiquitin C promoter. Cells were cultured in Dulbecco's modification of Eagle's medium (DMEM) supplemented with 10% FBS, 1% Glutamax, and 1% Pen-Strep at 37°C and 5% CO_2.

RNA extraction and Northern Blot

To extract total RNA from cell cultures, we added TRI reagent (or TRIzol) directly to the cells after removing the media and homogenized them by pipetting up and down (Rio et al., 2010). For RNA extraction from mouse organs, tissues were snap-frozen with liquid nitrogen and pulverized by mortar and pestle, followed by the addition of TRI reagent. RNA quality was assured via spectrophotometry and agarose gel electrophoresis.

For Northern blotting of β-actin mRNA, a total of 10-15 μg RNA was separated in 1.0% agarose gels and transferred to positively charged nylon membrane (Roche) using a semi-dry transfer kit (BioRad). After 30 min of prehybridization in SES1 solution (0.5 M Sodium phosphate, 7% (w/v) SDS, 1 mM EDTA, pH 7.2), the blot was incubated overnight with the ^{32}P end-labeled probes. For washing the membranes, 20×SSPE solution (3.6 M NaCl, 0.2 M NaH_2PO_4, 20 mM EDTA, pH 7.4) was prepared and diluted to 6×SSPE solution. After washing three times with 6×SSPE solution (30 min at 37℃ and twice more at 42℃), the membranes were placed in a phosphor screen cassette to obtain autoradiography images. The oligonucleotide probe sequences used in this study are as follows.

GSP1: CAAAACAATGTACAAAGTCCTCAGCCACATTTGTAGAACTTTGGGGGATG

GSP2: CCCAGGGAGACCAAAGCCTTCATACATCAAGTTGGGGGGACAAAAAAAAG

GSP3: ACATCAAGTTGGGGGGACAAAAAAAAGGGAGGCCTCAGACC

LK51: TTTCTAGGCAATTAGGTACCTTAGGATCTAATGAACCCGGGAATACTGCAG

Real-time quantitative polymerase chain reaction (RT-qPCR)

The WT and *Actb-MBS* MEF cells were cultured at a density of 2.2 x 10^6 cells per 100 mm dish followed by the addition of 100 μM DRB (5,6-Dichlorobenzimidazole 1-β-D-ribofuranoside)(Sigma). Total RNA was extracted from cells at different time points of the DRB treatment using the TRIzol reagent (Invitrogen) and then treated with DNase I (Roche) at 37℃ for 20 min to digest any genomic DNA followed by addition of 8 mM EDTA and heat-inactivation at 75℃ for 10 min. cDNA was prepared from the total mRNA by reverse transcription using TOPscript Reverse Transcriptase enzyme (enzynomics) with 100 μM random hexamers. The reaction was done with the SimpliAmp Thermal Cycler (Applied Biosystems) using the following cycling conditions: annealing at 25℃ for 10 min, reaction at 42℃ for 60 min and inactivation at 95℃ for 5 min.

A 2-step RT-qPCR reaction was done with 100 μM of each primer (mouse β-actin: FW 5′-CCACTGCCGCATCCTCTTCC-3′, REV 5′-CTCGTTGCCAATAGTGATGACCTG-3′; mouse GAPDH: FW 5′-CATGGCCTTCCGTGTTCCTA-3′, REV 5′-GCGGCACGTCAGATCCA-3′) and TOPreal qPCR 2× PreMIX (SYBR Green with high ROX) (enzynomics) using the StepOnePlus Real-Time PCR System (Thermo Fisher). Samples were run in triplicates and analyzed using the StepOnePlus Real-Time PCR software. β-actin mRNA levels were analyzed by the $2^{-\Delta\Delta Ct}$ method (Livak method) and normalized to the GAPDH mRNA levels.

RESULTS

To compare the size distribution of the labeled and unlabeled β-actin mRNA, we extracted RNA from the cells and tissues of WT, *Actb-MBS* (Lionnet et al., 2011), and MBS×MCP mice (Park et al., 2014). In the *Actb-MBS* mouse, the cassette containing 24 repeats of MBS (24×MBS) is knocked-in to the 3′UTR of the *Actb* gene 441 bp downstream of the stop codon and after the zipcode (Kislauskis et al., 1994) responsible for mRNA localization. The MCP mouse is a transgenic mouse that expresses MCP-GFP in every cell type. The *Actb-MBS* and MCP mice were crossed and bred to double homozygosity to generate the MBS×MCP mouse line (Park et al., 2014). In the MBS×MCP mouse, all endogenous β-actin mRNAs are labeled with up to 48 MCP-GFPs because each MBS binds a dimer of MCP-GFP. Previously, Lionnet *et al.* confirmed the successful knock-in of the 24×MBS and the proper size of the full-length modified mRNA transcript (Lionnet et al., 2011). The 24×MBS cassette is made of 12 repeats of a tandem MBS doublet unit. Each unit has two 19-ribonucleotide (nt)-long stem-loops that are connected by a 20-nt spacer, and a 51-nt linker connects the doublet units. For the Northern blot analysis, we used three gene-specific probes that hybridize to the 5′ side (GSP1) and the 3′ side (GSP2 and GSP3) of the 24×MBS cassette and the LK51 probe that hybridizes to the 51-nt linker (Fig. 1). Because of the lower sequence specificity of GSP2 and GSP3, we designed two probes for the 3′ side of the 24×MBS cassette. While each GSP probe has only one hybridization site in the β-actin transcript, the LK51 probe has 11 hybridization sites in the modified full-length mRNA, providing a higher signal intensity and sensitivity.

First, we compared the Northern blot images of the immortalized MEF cell lines obtained from the WT, homozygous *Actb-MBS*, and double homozygous MBS×MCP mice (Fig. 2). Unlike the yeast model studies (Garcia and Parker, 2015, 2016), we could not observe the accumulation of the 3′ decay products in any of the three cell lines. Some smearing due to general RNA degradation was observed with the LK51 and 18S rRNA probes because they had a much stronger signal than that of the GSP probes (Fig. 2A). However, there were no noticeable 3′ decay fragments that hybridized with the GSP2 probe in either the *Actb-MBS* or MBS×MCP MEF cell lines compared with the WT MEF. By increasing the photomultiplier tube (PMT) voltage, we confirmed that little difference was found in the degradation patterns of the labeled and unlabeled β-actin transcripts (Fig. 2B). The overall stability of the WT and MBS labeled β-actin mRNA was also similar to each other at different time points after inhibition of transcription by DRB ($p \leq 0.05$ by ANOVA, Fig. 2C).

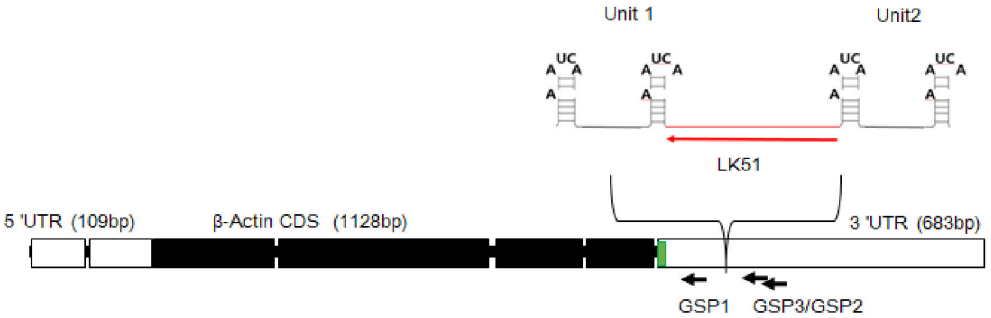

Fig. 1. Schematic of Northern blot probe sites on the endogenous and 24×MBS-tagged β-actin mRNA. The 24×MBS cassette is inserted within the 3′UTR of β-actin mRNA, downstream of the zipcode (green) after the stop codon. The hybridization sites of the GSP probes (black arrows) are on the 5′ side (GSP1) or 3′ side (GSP2 and GSP3) of the 24×MBS insertion position. The 24×MBS cassette has 11 linkers that connect 12 units of the double stem-loops. Each of the 11 linkers is a hybridization site of the LK51 probe (red arrow).

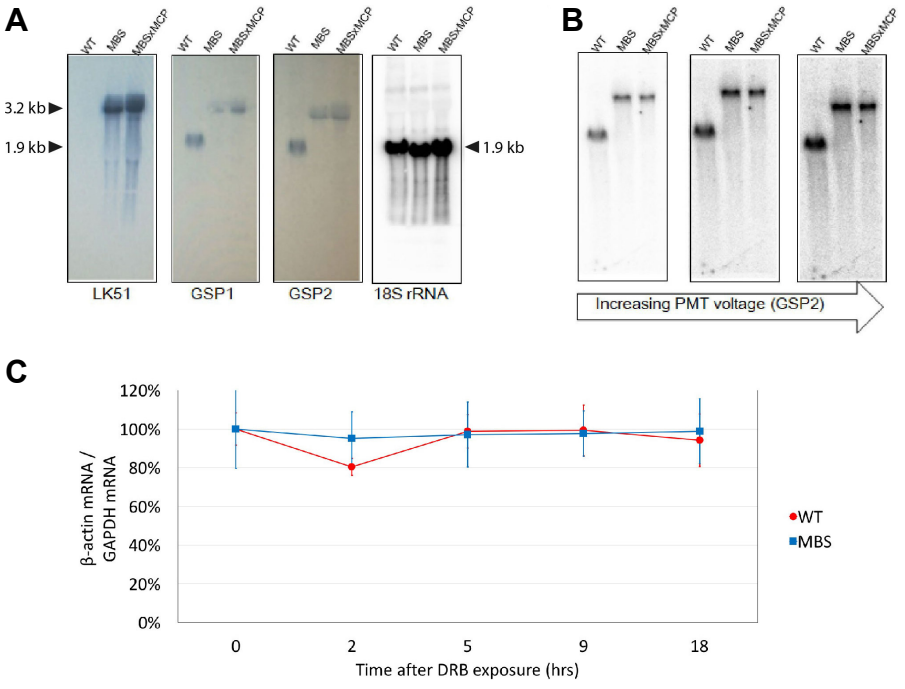

Fig. 2. Comparison of WT and MS2-labeled endogenous β-actin mRNA in the immortalized MEF cell lines. (A) Northern blot of β-actin mRNA from WT, *Actb-MBS* (MBS), and MBS×MCP MEFs probed with LK51, GSP1, and GSP2 probes. An 18S rRNA probe was used as a total RNA loading control. The sizes of WT and MS2-labeled β-actin mRNA (1.9 kb and 3.2 kb, respectively) as well as the size of 18S rRNA (1.9 kb) are indicated. (B) Northern blot images of the GSP2 probe with increasing photomultiplier tube (PMT) voltage. (C) Relative levels of β-actin mRNA normalized by GAPDH mRNA at different time points after DRB treatment of WT and MBS MEFs (n = 3). Error bars represent the double standard error of the mean (± 2×SE).

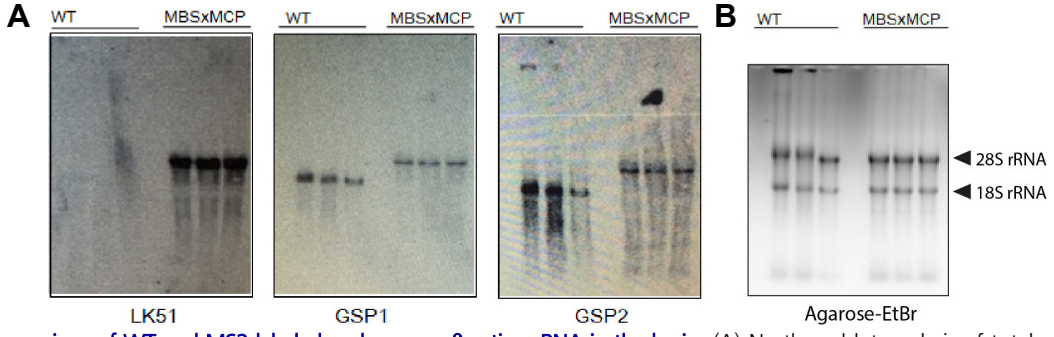

Fig. 3. Comparison of WT and MS2-labeled endogenous β-actin mRNA in the brain. (A) Northern blot analysis of total mRNA extracts from WT and MBS×MCP mouse brains with LK51, GSP1, and GSP2 probes. (B) Ethidium bromide (EtBr)-stained agarose gel image of total mRNA extracts from WT and MBS×MCP mouse brains. Each lane represents mRNA from each mouse (n = 3).

Next, we performed Northern blot analysis for whole brain lysates from the WT and MBS×MCP mice. We randomly chose three mice from each group and sacrificed them to obtain brain samples. The total RNA extract from the brain samples were probed with the LK51, GSP1, and GSP2 probes (Fig. 3). There was no noticeable difference between the WT and the MS2-GFP-labeled β-actin mRNA transcripts in the brain tissue samples.

Finally, we examined the β-actin mRNA degradation patterns in several different organs from the WT, *Actb-MBS*, and MBS×MCP mice. Again, no clear organ-specific feature was noted in regard to the integrity of the mRNA (Fig. 4). Six mouse organs, including brain, testis, kidney, liver, heart, and lung, showed no noticeable accumulation of the mRNA decay product in the *Actb-MBS* and MBS×MCP mouse lines compared with the WT mice. This finding confirmed that MCP-GFP binding negligibly influences the RNA decay in this mouse model system.

DISCUSSION

In this report, we examined the size distribution of MS2-GFP labeled β-actin mRNAs that were endogenously expressed in murine cells and tissues. Although recent studies in budding yeast models have raised concerns about aberrant mRNA degradation upon MS2-GFP labeling (Garcia and Parker, 2015, 2016; Haimovich et al., 2016; Heinrich et al., 2017), we did not find such accumulation of mRNA decay fragments in the *Actb-MBS* knock-in and MBS×MCP mice.

While we were preparing this report, Tuttucci et al. introduced a newer version of MBS called MBSV6 (Tutucci et al., 2018b). MBSV6 has a uridine (U) at position -5 of the

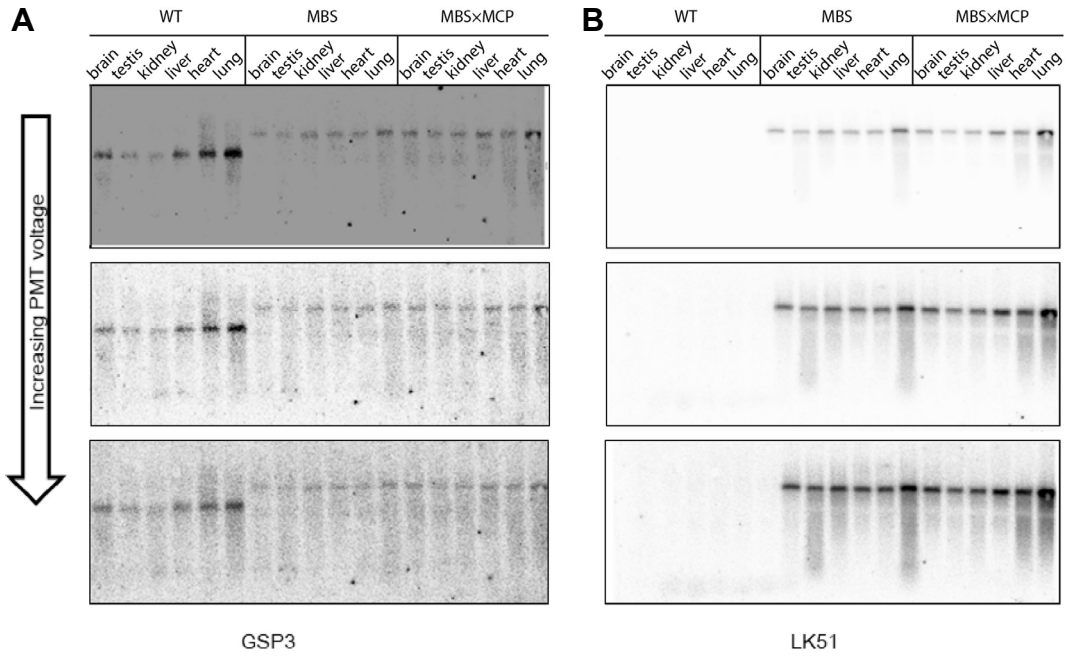

Fig. 4. Northern blot of β-actin mRNA from various mouse organs. (A) Total RNAs from six organ samples of brain, testis, kidney, liver, heart, and lung, from WT, *Actb-MBS* (MBS), and MBS×MCP mice were probed with GSP3. (B) The same membrane shown in (A) was stripped and probed again with LK51. The membrane was scanned with increasing PMT voltage from the top to the bottom panels.

loop instead of a cytosine (C) in the previous versions of MBS. The C-to-U replacement reduced the binding affinity between the stem-loop sequence and MCP by 10-fold, which prevented the accumulation of mRNA decay fragments in yeasts. MBSV6 was successfully used for tagging both constitutively expressed mRNAs (*MDN1* and *DOA1*) and highly regulated mRNAs (*GAL1* and *ASH1*) without affecting their normal degradation pattern. Therefore, the use of MBSV6 is preferable for single RNA imaging in yeasts. However, in mammalian cells, the authors did not observe MBS aggregates using either the old or the new version of MBS. Additionally, Horvathova *et al.* showed that the MS2 and PP7 stem-loops bound to their respective coat proteins did not stabilize any degradation intermediate of the reporter mRNA in HeLa cells (Horvathova et al., 2017).

Because mRNA is relatively short-lived in bacteria and yeasts, degradation of MBS could be rate-limiting for the decay of the labeled mRNA (Tutucci et al., 2018b). The average half-life of mRNA in *E. coli* is approximately 5 min (Moran et al., 2013) and that in *S. cerevisiae* is approximately 23 min (Wang et al., 2002). However, the half-lives of most mRNAs in mammalian cells are much longer. The median half-life of mRNA in mouse embryonic stem cells is approximately 7.1 hours (Sharova et al., 2009) and that in human cells is approximately 10 hours (Yang et al., 2003). In particular, β-actin mRNA is well-known to be stable with a half-life of 9 hours (Reuner et al., 1995). Because of the longer half-lives of mRNAs in general, MS2-GFP labeling may be less prone to the accumulation of decay fragments in mammalian cells.

In addition to the lifetime of mRNA, the expression level and the insertion position of the MBS cassette are important factors to consider when using the MS2-GFP tagging system. Both the Parker and Gerst groups agreed that overexpression of MS2-labeled mRNAs caused the accumulation of 3′ decay fragments (Garcia and Parker, 2015; Haimovich et al., 2016). The insertion position of the MBS cassette is typically chosen in the 3′UTR to minimize any perturbation in the transcription and translation of the mRNA. However, there are many cis-regulatory elements and trans-acting factors in the 3′UTR, the disruption of which may cause the mislocalization of the mRNA and dysregulation of mRNA stability. Because the same tagging method could work differently under the context of the experiment, e.g., the model organism, target mRNA species, and the labeling site, it is important to verify whether the labeled mRNA faithfully recapitulates the behavior of the original molecule before further extensive and costly analysis.

In summary, we have confirmed that the *Actb-MBS* knock-in and MBS×MCP hybrid mouse models can be used to image the dynamics of β-actin mRNA without the worrisome accumulation of mRNA decay fragments. Using Northern blot analysis, we examined the integrity of the labeled mRNA in immortalized mouse embryonic cell lines and various organ tissues. In addition to Northern blot, other experimental techniques, such as single molecule FISH and RT-qPCR, have been used to validate the MS2 and other orthologous tagging systems (Das et al., 2018; Haimovich et al., 2016; Heinrich et al., 2017; Lionnet et al., 2011; Tutucci et al., 2018b). Various fluorescent RNA tagging methods are being continuously developed and refined to visualize diverse biological phenomena in living cells. As exemplified by

the MS2-GFP system, it is imperative to validate the labeling technique in the context of each study. Single RNA imaging, when conducted with caution, has much potential to reveal a thus-far unrecognized complexity in the life-long path of RNA inside a cell.

ACKNOWLEDGMENTS

This work was supported by the Creative-Pioneering Researchers Program through Seoul National University and the Howard Hughes Medical Institute (HHMI)-Wellcome International Scholar Awards from the Wellcome Trust [208468/Z/17/Z].

REFERENCES

Beach, D.L., Salmon, E.D., and Bloom, K. (1999). Localization and anchoring of mRNA in budding yeast. Curr. Biol. *9*, 569-578.

Bertrand, E., Chartrand, P., Schaefer, M., Shenoy, S.M., Singer, R.H., and Long, R.M. (1998). Localization of ASH1 mRNA particles in living yeast. Mol. Cell *2*, 437-445.

Buxbaum, A.R., Wu, B., and Singer, R.H. (2014). Single beta-actin mRNA detection in neurons reveals a mechanism for regulating its translatability. Science *343*, 419-422.

Cho, W.K., Jayanth, N., English, B.P., Inoue, T., Andrews, J.O., Conway, W., Grimm, J.B., Spille, J.H., Lavis, L.D., Lionnet, T., et al. (2016). RNA Polymerase II cluster dynamics predict mRNA output in living cells. Elife *5*, e13617.

Das, S., Moon, H.C., Singer, R.H., and Park, H.Y. (2018). A transgenic mouse for imaging activity-dependent dynamics of endogenous Arc mRNA in live neurons. Sci. Adv. *4*, eaar3448.

Eliscovich, C., Shenoy, S.M., and Singer, R.H. (2017). Imaging mRNA and protein interactions within neurons. Proc. Natl. Acad. Sci. USA *114*, E1875-E1884.

Fusco, D., Accornero, N., Lavoie, B., Shenoy, S.M., Blanchard, J.M., Singer, R.H., and Bertrand, E. (2003). Single mRNA molecules demonstrate probabilistic movement in living mammalian cells. Curr. Biol. *13*, 161-167.

Garcia, J.F., and Parker, R. (2015). MS2 coat proteins bound to yeast mRNAs block 5′ to 3′ degradation and trap mRNA decay products: implications for the localization of mRNAs by MS2-MCP system. RNA *21*, 1393-1395.

Garcia, J.F., and Parker, R. (2016). Ubiquitous accumulation of 3′ mRNA decay fragments in *Saccharomyces cerevisiae* mRNAs with chromosomally integrated MS2 arrays. RNA *22*, 657-659.

Golding, I., and Cox, E.C. (2004). RNA dynamics in live *Escherichia coli* cells. Proc. Natl. Acad. Sci. USA *101*, 11310-11315.

Grunwald, D., and Singer, R.H. (2010). *In vivo* imaging of labelled endogenous beta-actin mRNA during nucleocytoplasmic transport. Nature *467*, 604-607.

Haimovich, G., Zabezhinsky, D., Haas, B., Slobodin, B., Purushothaman, P., Fan, L., Levin, J.Z., Nusbaum, C., and Gerst, J.E. (2016). Use of the MS2 aptamer and coat protein for RNA localization in yeast: A response to "MS2 coat proteins bound to yeast mRNAs block 5′ to 3′ degradation and trap mRNA decay products: implications for the localization of mRNAs by MS2-MCP system". RNA *22*, 660-666.

Heinrich, S., Sidler, C.L., Azzalin, C.M., and Weis, K. (2017). Stem-loop RNA labeling can affect nuclear and cytoplasmic mRNA processing. RNA *23*, 134-141.

Horvathova, I., Voigt, F., Kotrys, A.V., Zhan, Y., Artus-Revel, C.G., Eglinger, J., Stadler, M.B., Giorgetti, L., and Chao, J.A. (2017). The dynamics of mRNA turnover revealed by single-molecule imaging in single cells. Mol. Cell *68*, 615-625.

Kalo, A., Kanter, I., Shraga, A., Sheinberger, J., Tzemach, H., Kinor, N., Singer, R.H., Lionnet, T., and Shav-Tal, Y. (2015). Cellular levels of signaling factors are sensed by beta-actin alleles to modulate transcriptional pulse intensity. Cell Rep. *13*, 1284-1285.

Katz, Z.B., English, B.P., Lionnet, T., Yoon, Y.J., Monnier, N., Ovryn, B., Bathe, M., and Singer, R.H. (2016). Mapping translation 'hot-spots' in live cells by tracking single molecules of mRNA and ribosomes. Elife *5*, e10415.

Katz, Z.B., Wells, A.L., Park, H.Y., Wu, B., Shenoy, S.M., and Singer, R.H. (2012). beta-Actin mRNA compartmentalization enhances focal adhesion stability and directs cell migration. Genes Dev. *26*, 1885-1890.

Kislauskis, E.H., Zhu, X., and Singer, R.H. (1994). Sequences responsible for intracellular localization of beta-actin messenger RNA also affect cell phenotype. J. Cell Biol. *127*, 441-451.

Lee, B.H., and Park, H.Y. (2018). HybTrack: A hybrid single particle tracking software using manual and automatic detection of dim signals. Sci. Rep. *8*, 212.

Lionnet, T., Czaplinski, K., Darzacq, X., Shav-Tal, Y., Wells, A.L., Chao, J.A., Park, H.Y., de Turris, V., Lopez-Jones, M., and Singer, R.H. (2011). A transgenic mouse for *in vivo* detection of endogenous labeled mRNA. Nat. Methods *8*, 165-170.

Monnier, N., Barry, Z., Park, H.Y., Su, K.C., Katz, Z., English, B.P., Dey, A., Pan, K., Cheeseman, I.M., Singer, R.H., et al. (2015). Inferring transient particle transport dynamics in live cells. Nat. Methods *12*, 838-840.

Moon, H.C., Lee, B.H., Lim, K., Son, J.S., Song, M.S., and Park, H.Y. (2016). Tracking single mRNA molecules in live cells. J. Phys. D Appl. Phys. *49*, 233001.

Moran, M.A., Satinsky, B., Gifford, S.M., Luo, H., Rivers, A., Chan, L.K., Meng, J., Durham, B.P., Shen, C., Varaljay, V.A., et al. (2013). Sizing up metatranscriptomics. ISME J. *7*, 237-243.

Park, H.Y., Buxbaum, A.R., and Singer, R.H. (2010). Single mRNA tracking in live cells. Methods Enzymol. *472*, 387-406.

Park, H.Y., Lim, H., Yoon, Y.J., Follenzi, A., Nwokafor, C., Lopez-Jones, M., Meng, X., and Singer, R.H. (2014). Visualization of dynamics of single endogenous mRNA labeled in live mouse. Science *343*, 422-424.

Park, H.Y., Trcek, T., Wells, A.L., Chao, J.A., and Singer, R.H. (2012). An unbiased analysis method to quantify mRNA localization reveals its correlation with cell motility. Cell Rep. *1*, 179-184.

Rath, A.K., and Rentmeister, A. (2015). Genetically encoded tools for RNA imaging in living cells. Curr. Opin. Biotechnol. *31*, 42-49.

Reuner, K.H., Wiederhold, M., Dunker, P., Just, I., Bohle, R.M., Kroger, M., and Katz, N. (1995). Autoregulation of actin synthesis in hepatocytes by transcriptional and posttranscriptional mechanisms. Eur. J. Biochem. *230*, 32-37.

Rio, D.C., Ares, M., Jr., Hannon, G.J., and Nilsen, T.W. (2010). Purification of RNA using TRIzol (TRI reagent). Cold Spring Harb Protoc. *2010*, pdb prot5439.

Sharova, L.V., Sharov, A.A., Nedorezov, T., Piao, Y., Shaik, N., and Ko, M.S. (2009). Database for mRNA half-life of 19 977 genes obtained by DNA microarray analysis of pluripotent and differentiating mouse embryonic stem cells. DNA Res. *16*, 45-58.

Slobodin, B., and Gerst, J.E. (2010). A novel mRNA affinity purification technique for the identification of interacting proteins and transcripts in ribonucleoprotein complexes. RNA *16*, 2277-2290.

Smith, C.S., Preibisch, S., Joseph, A., Abrahamsson, S., Rieger, B., Myers, E., Singer, R.H., and Grunwald, D. (2015). Nuclear accessibility of beta-actin mRNA is measured by 3D single-molecule real-time tracking. J. Cell Biol. *209*, 609-619.

Song, M.S., Moon, H.C., Jeon, J.H., and Park, H.Y. (2018). Neuronal messenger ribonucleoprotein transport follows an aging Levy walk. Nat. Commun. *9*, 344.

Tutucci, E., Livingston, N.M., Singer, R.H., and Wu, B. (2018a). Imaging mRNA *in vivo*, from birth to death. Annu. Rev. Biophys. *47*, 85-106.

Tutucci, E., Vera, M., Biswas, J., Garcia, J., Parker, R., and Singer, R.H. (2018b). An improved MS2 system for accurate reporting of the mRNA life cycle. Nat. Methods *15*, 81-89.

Vera, M., Biswas, J., Senecal, A., Singer, R.H., and Park, H.Y. (2016). Single-cell and single-molecule analysis of gene expression regulation. Annu. Rev. Genet. *50*, 267-291.

Wang, Y., Liu, C.L., Storey, J.D., Tibshirani, R.J., Herschlag, D., and Brown, P.O. (2002). Precision and functional specificity in mRNA decay. Proc. Natl. Acad. Sci. USA *99*, 5860-5865.

Wu, B., Buxbaum, A.R., Katz, Z.B., Yoon, Y.J., and Singer, R.H. (2015). Quantifying protein-mRNA interactions in single live cells. Cell *162*, 211-220.

Yang, E., van Nimwegen, E., Zavolan, M., Rajewsky, N., Schroeder, M., Magnasco, M., and Darnell, J.E., Jr. (2003). Decay rates of human mRNAs: correlation with functional characteristics and sequence attributes. Genome Res. *13*, 1863-1872.

Yoon, Y.J., Wu, B., Buxbaum, A.R., Das, S., Tsai, A., English, B.P., Grimm, J.B., Lavis, L.D., and Singer, R.H. (2016). Glutamate-induced RNA localization and translation in neurons. Proc. Natl. Acad. Sci. USA *113*, E6877-E6886.